

Multi-frequency spectral analysis of extragalactic radio sources in the 33-GHz VSA catalogue: sources with flattening and upturn spectrum.

M. Tucci¹, J.A. Rubiño-Martin¹, R. Rebolo¹, R. Genova-Santos², R.A. Watson³, R.A. Battye³, K.A. Cleary⁴, R.D. Davies³, R.J. Davis³, K. Grainge², M. Hobson², R.D.E. Saunders², A. Scaife², P.F. Scott²

¹*Instituto de Astrofísica de Canarias, 38200 La Laguna, Tenerife, Canary Islands, Spain*

²*Astrophysics Group, Cavendish Laboratory, University of Cambridge, Madingley Road, Cambridge CB3 0HE*

³*Jodrell Bank Observatory, University of Manchester, Macclesfield, Cheshire SK11 9DL*

⁴*California Institute of Technology, 1200 E California Blvd, Pasadena, CA 91125*

ABSTRACT

We present an analysis of the spectral properties of the extragalactic radio sources in the nearly-complete VSA sample at 33 GHz. Data from different surveys are used to study source spectra between 1.4 and 33 GHz. We find that, in general, spectra can not be well described by a single power law in the range of frequencies considered. In particular, most of the VSA sources that are steep between 1.4 and 5 GHz, show a spectral flattening at $\nu > 5$ GHz. We identify 20 objects (19% of the sample) clearly characterized by an upturn spectrum, i.e., a spectrum falling at low frequencies ($\nu \lesssim 5$ GHz) and inverted at higher frequencies. Spectra with high-frequency flattening or upturn shape are supposed to occur when the emission from the AGN compact core begins to dominate over the component from extended lobes. This picture fits well with the AGN unified scheme, for objects observed at intermediate viewing angles of the AGN jet. Finally, we discuss implications that this class of sources can have on future CMB observations at high resolution.

Key words:

Galaxies: active – quasars: general; Radio continuum: galaxies; Cosmic microwave background

1 INTRODUCTION

In recent years, extragalactic radio sources have received increased attention due to their contamination of the cosmic background radiation (CMB) temperature fluctuations and polarization on small angular scales (Toffolatti et al. 2005; Tucci et al. 2004). At microwave wavelengths, this contribution is dominated by objects powered by active galactic nuclei (AGNs), such as quasars or BL Lacs. These sources are usually separated according to the slope of the spectrum at GHz frequencies (usually assumed a power law; hereafter $S \propto \nu^\alpha$): steep-spectrum if the spectral index $\alpha \leq -0.5$ and flat-spectrum otherwise. The sources are thus divided into two classes, corresponding approximately to those where the radio flux is predominantly emitted from the extended lobes and those where the compact core is the brightest component (Peacock 1985).

Based on this scheme, evolutionary models for ra-

dio sources provide accurate predictions for the number counts at frequencies $\nu \lesssim 8$ GHz and down to flux densities of fractions of mJy (Dunlop & Peacock 1990; Toffolatti et al. 1998; Jackson & Wall 1999; De Zotti et al. 2005). Recently, De Zotti et al. (2005) updated and improved evolutionary models taking into accounts new high-frequency data from the 15-GHz 9C (Waldram et al. 2003), 18-GHz ATCA catalogues (Ricci et al. 2004) and WMAP (first year; Bennett et al. 2003). However, estimates of the radio source contribution to temperature fluctuations at cm/mm wavelengths, i.e. at wavelengths interesting for CMB observations, is still problematic. In fact, radio spectra of AGNs can be much more complex than a single power law, that may not provide a satisfactory description in a wide range of frequencies (see, e.g., simultaneous multi-frequency measurements of radio spectra by Trushkin 2003 and Bolton et al. 2004). Different mechanisms can be responsible for this: (i) a spectral steepening is expected due

to the more rapid energy loss of high-energy electrons with source age; (ii) a transition from optically thick to optically thin regimes can occur at high frequencies; (iii) at different wavelengths radio emission can be dominated by different components characterised by a distinct spectral behaviour. For example, AGNs with spectra peaked at GHz frequencies (GPS) are well known, while objects with spectra still inverted at frequencies as high as 20–30 GHz are expected to fall at some peak frequency (see O’Dea 1998 and De Zotti et al. 2005 for reviews on GPS and extreme GPS sources).

Recently, indications of a class of radio sources with spectra that are “opposite” in respect to the GPS ones, are appearing in the literature. Sadler et al. (2006), using multi-frequency data of the ATCA 20-GHz pilot survey, observed objects with spectrum falling at low frequencies, but turning up and beginning to rise around 5 GHz, and called them “upturn” sources. They found that about 20% of the sources belongs to this class. Trushkin (2003) identified in the first-year WMAP source catalogue 15 sources (corresponding to 7%) with “combined spectra with a power low-frequency component and a flat (inverse) high-frequency component”. Upturn objects are observed also in recent observations by ATCA (Massardi et al. 2007; Sadler et al. 2007) and by Partridge et al. (2007) in nearby galaxy clusters.

The presence of a significant fraction of upturn sources in samples selected at few tens of GHz could have important implications for CMB observations and for models predicting the radio source contribution at CMB frequencies. These sources, in fact, could appear in high-frequency surveys with flux densities much brighter than expected from low-frequency extrapolations.

In this paper we carry out a multi-frequency spectral analysis of the sources detected by the extended version of the Very Small Array (VSA) at 33 GHz (Cleary et al. 2005, C05 hereafter). VSA provides a deep and nearly-complete survey of extragalactic radio sources with a flux limit of 20 mJy. A first discussion on the spectrum of these sources and their variability was carried out by C05, with an estimate of the source number counts at 33 GHz in the flux range 20–114 mJy. Here, we exploit surveys at different frequencies, as the NRAO VLA Sky Survey (NVSS, Condon et al. 1998) at 1.4 GHz, the Green Bank survey (GB6, Gregory et al. 1996) at 4.8 GHz and the Ryle Telescope (RT, Waldram et al. 2003) at 15 GHz, in order to study the spectrum of VSA radio sources in a quite extended range of frequencies. In particular, we focus our attention on sources whose spectrum shows a high-frequency flattening or an upturn behaviour, discussing a physical interpretation for such spectra.

2 THE VSA SOURCE CATALOGUE

The Very Small Array (VSA) consists of a 14-element interferometer operating in the band 26–36 GHz, located at Teide Observatory in Tenerife (see, e.g., Watson et al. 2003). Two 3.7 m antennas, spaced 9.2 m apart (called the “source subtractor”), are used to measure the flux density of sources present in the VSA fields. The sources to be followed by the subtractor are preselected from a catalogue at 15 GHz provided by the Ryle Telescope (RT, see e.g. Jones 1991 and

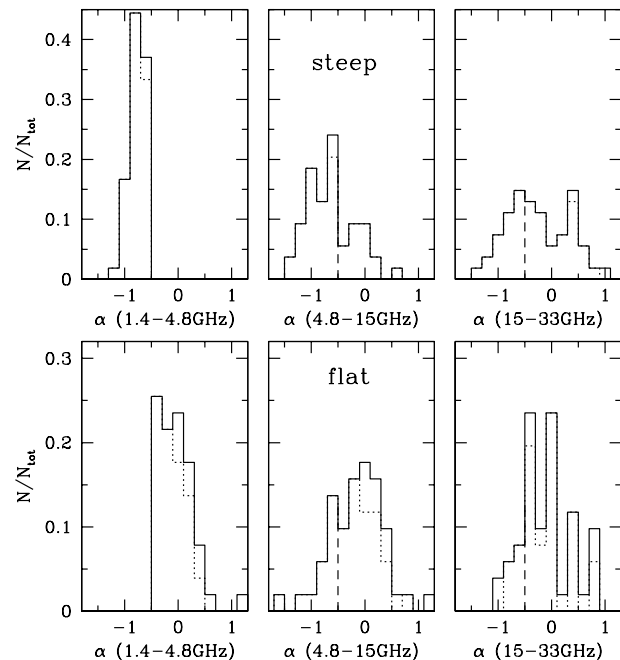


Figure 1. Distribution of spectral indices for steep- and flat-spectrum (defined between [1.4, 4.8] GHz) sources, calculated in frequency ranges [1.4, 4.8] GHz, [4.8, 15] GHz and [15, 33] GHz. Dotted histograms are excluding sources without 4.8-GHz measurements. Vertical dashed lines correspond to $\alpha = -0.5$.

Waldram et al. 2003) that surveyed the VSA fields in advance of CMB observations. For the extended configuration of the VSA (Grainge et al. 2003; Dickinson et al. 2004) it was required that all sources with flux $S \gtrsim 20$ mJy were subtracted from CMB maps produced by the VSA main array. In order to satisfy this goal, the source subtractor followed all the sources detected by RT in the VSA fields up to the RT flux limit of 2 mJy. This ensures that all sources (except for extremely inverted ones) with $S \gtrsim 20$ mJy at 33 GHz are observed by the source subtractor (C05).

Our analysis is based on the catalogue of extragalactic radio sources presented by C05 and used to estimate the number counts at 33 GHz and to correct the source contribution to the VSA extended array power spectrum (see also Dickinson et al. 2004). Due to errors in the text of Table A1 in C05, we use the list of 33-GHz sources from Cleary et al. (2008). The catalogue consists of 102 sources with flux density between 20 and 114 mJy, within well-defined regions of the VSA fields that cover a total area of 0.044 sr. We consider also 3 further objects present in the VSA area and brighter than 114 mJy. All these sources satisfy the pre-selection condition to be brighter than 10 mJy at 15 GHz. As a consequence, the sample can not be considered strictly complete because there is the possibility that some sources with rising spectral index between 15 and 33 GHz ($\alpha_{15}^{33} \gtrsim 1$) and $S_{33} \gtrsim 20$ mJy exist in the VSA fields but it is not present in the sample. However, such inverted sources are rare and the loss of few of them would not affect the following analysis.

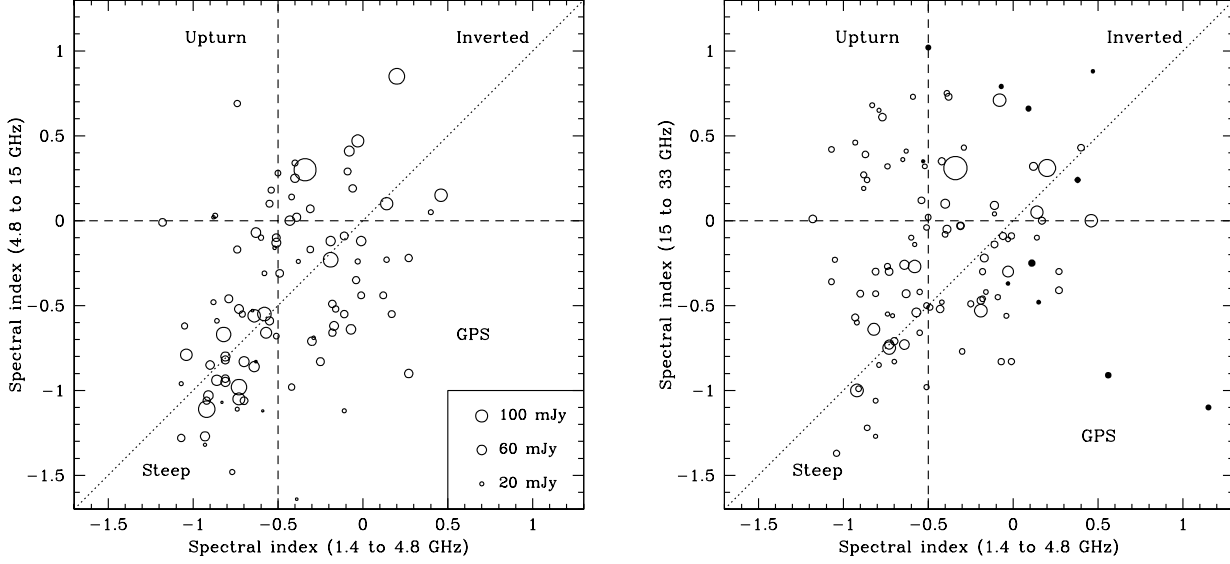


Figure 2. “Two colour diagrams”: the spectral index calculated at intermediate (left plot) and high (right plot) frequencies vs the value at low frequencies. The size of the circle is related to the flux density at 15 GHz (left plot) and at 33 GHz (right plot). The vertical dashed line divides sources into steep- and flat-spectrum. Full dots in the right plot correspond to sources without 4.8 GHz flux; in this case, $\alpha_{1.4}^{4.8}$ is substituted with $\alpha_{1.4}^{15}$.

3 SPECTRAL PROPERTIES IN THE FREQUENCY RANGE [1.4, 33] GHz

Spectral properties of sources in the VSA sample can be studied using flux densities from surveys at lower frequencies: at 15 GHz from the RT; at 4.8 GHz from the GB6; and at 1.4 GHz from the NVSS. Only 11 objects do not have a counterpart in the GB6 survey, most of them characterized by an inverted spectrum between 1.4 and 15 GHz and a low flux density at 1.4 GHz. We separate VSA sources into steep- and flat-spectrum sources according to their spectral index between 1.4 and 4.8 GHz (or 15 GHz in the case that 4.8-GHz flux density is not available). The sample is almost equally divided into steep- and flat-spectrum sources, being 54 and 51 respectively, as predicted by evolutionary models for radio sources in this flux-density range (see, e.g., De Zotti et al. 2005).

Figure 1 shows the distribution of spectral indices for the two source populations in three different intervals of frequencies: [1.4, 4.8] GHz, [4.8, 15] GHz and [15, 33] GHz (hereafter indicated as low, intermediate and high frequencies respectively). We suppose $\alpha_{1.4}^{4.8} = \alpha_{4.8}^{15} = \alpha_{15}^{33}$ for the 11 sources without measurements at 5 GHz. For **flat-spectrum sources**, the dispersion in the distribution of spectral indices increases at intermediate and high frequencies, with tails up to strongly inverted or steep indices ($|\alpha| \gtrsim 1$). However, the average value of α remains nearly constant with the frequency interval,

$$\langle \alpha_{1.4}^{4.8} \rangle = -0.05 \quad \langle \alpha_{4.8}^{15} \rangle = -0.15 \quad \langle \alpha_{15}^{33} \rangle = -0.11$$

Different remarks can be drawn for **steep-spectrum sources**. The distribution of $\alpha_{1.4}^{4.8}$ is very peaked between -1 and -0.5, as expected because very steep-spectrum sources have low probability to be observed at high frequency. In the

intermediate interval spectral indices spread both to positive and to very steep values, but keeping a similar average α . On the contrary, a clear “flattening” in spectra is observed at high frequencies, where more than 60% of sources have $\alpha_{15}^{33} > -0.5$ and 1/3 of steep sources has become inverted; the average value increases by +0.5 from the low- to the high-frequency interval:

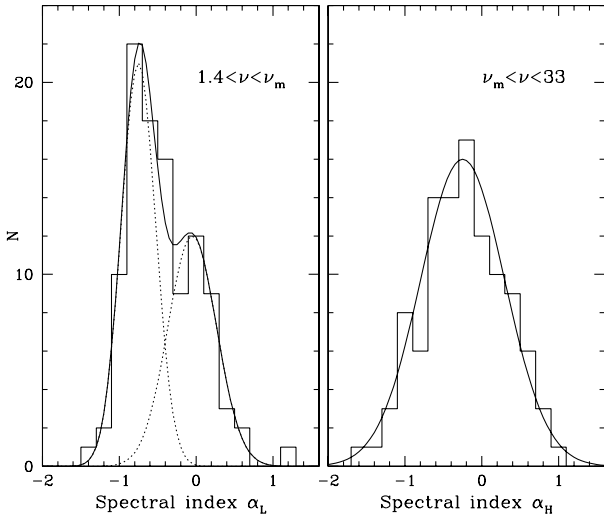
$$\langle \alpha_{1.4}^{4.8} \rangle = -0.75 \quad \langle \alpha_{4.8}^{15} \rangle = -0.65 \quad \langle \alpha_{15}^{33} \rangle = -0.25$$

The presence of curvatures in source spectra is more evident in “two-colour diagrams”: in Figure 2 we compare the low-frequency spectral index, $\alpha_{1.4}^{4.8}$, with the one obtained at higher frequencies. In the left plot of Figure 2, we have $\alpha_{4.8}^{15}$ vs $\alpha_{1.4}^{4.8}$: spectral indices seem to be distributed around the line $\alpha_{4.8}^{15} = \alpha_{1.4}^{4.8}$, with a bigger dispersion for flat-spectrum sources. Only in a few objects does the spectral index significantly change. No systematic trends can be observed and a single power law could statistically describe source spectra. This is not the case when we consider the high-frequency spectral index (α_{15}^{33} vs $\alpha_{1.4}^{4.8}$; see right plot). In most of the steep-spectrum sources the spectrum tends to flatten at high frequency or even to become inverted (i.e. with the typical upturn shape). For flat-spectrum sources we notice a clear flattening only in objects with spectral index $-0.5 < \alpha_{1.4}^{4.8} < -0.3$, that represent a transition from proper steep-spectrum (lobe-dominated AGN) and flat-spectrum (core-dominated AGN) sources. In general, if we consider sources with $\alpha_{1.4}^{4.8} \gtrsim -0.3$, there is an average steepening in spectra at $\nu > 5$ GHz and very few objects keep the spectrum flat or inverted at high frequencies.

The radius of circles in Figure 2 is related to the flux density of sources: a visual inspection of the plots does not show any correlation between the position of sources in the two-colour plot and their flux density. To confirm this, we

Table 1. Number of sources with $|\Delta\alpha| = |\alpha_H - \alpha_L| > 0.3$ (in brackets, > 0.5).

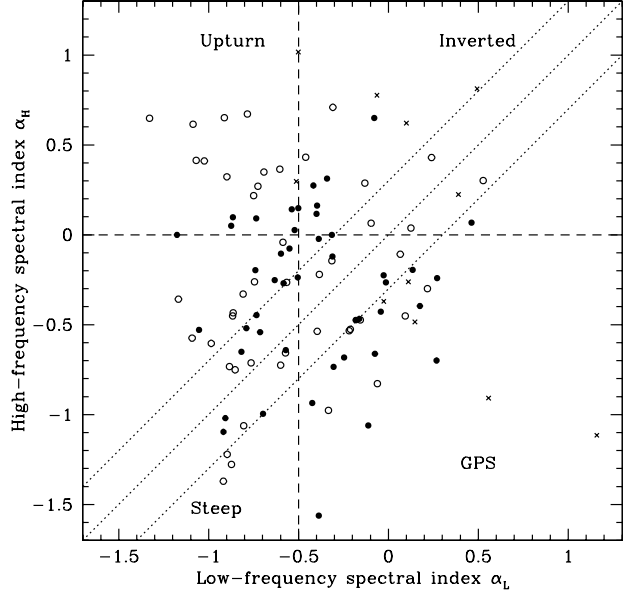
α_H vs α_L						
α_L	N	steeper	flatter	upturn	GPS	$\langle\alpha\rangle$
≤ -0.5	53	3 (0)	35 (25)	19	–	0.55
$(-0.5, -0.3]$	16	4 (3)	8 (6)	6	–	0.16
> -0.3	36	21 (11)	5 (3)	2	10	-0.33

**Figure 3.** Distribution of spectral indices at low (left plot) and high (right plot) frequencies. Solid lines are the Gaussian fit of the distributions.

calculate the *linear correlation coefficient* r between the flux density at 33 GHz, S_{33} , and the spectral index variation $\alpha_{15}^{33} - \alpha_{1.4}^{4.8}$: using all the sample, we find $r = 0.027$ with a probability for the null hypothesis of zero correlation of 0.76. This probability increases up to 0.8 (0.96) if we consider only sources with $\alpha_{1.4}^{4.8} < 0$ (< -0.3). This is particularly important because the lack of correlation rules out that spectral flattening at high frequencies occurs only in faint objects, where uncertainties in flux densities are higher: as example, we find that the brightest source of the sample (source 1734+3857) have $\alpha_{15}^{33} \gtrsim \alpha_{4.8}^{15} \gg \alpha_{1.4}^{4.8}$. Moreover, a correlation between 33-GHz flux densities and spectral flattening should be expected if flattening is observed in objects that are just in the extreme of the spectral index distribution.

3.1 Fit by two power law of source spectra

For a better characterization of source spectra and their curvature (when present), we suppose spectra to be well described by two different power laws. Let ν_m be the frequency at which the change in the spectral slope occurs. We define the low-frequency (α_L) and the high-frequency (α_H) spectral indices as the indices of the two best-fit power laws between $[1.4, \nu_m]$ GHz and $[\nu_m, 33]$ GHz respectively. The first step is to find out the frequency ν_m at which source spectra

**Figure 4.** Two colour diagram using spectral indices from two-power-law best fit. Open points are for objects whose α_H is calculated between 15 and 33 GHz; solid points for objects whose α_H is calculated between 4.8 and 33 GHz; crosses for objects without 4.8-GHz measurements. The diagonal dotted lines represent $\alpha_H = \alpha_L + 0.3/0.3$ respectively.

are better fitted, considering that, in our case, ν_m can only be 4.8 or 15 GHz. Figure 3 shows the distribution of α_L and α_H of the VSA sources. The former presents a bimodal distribution that can be fitted by two Gaussian distributions of mean -0.75 and -0.05 and dispersion 0.22 and 0.32 respectively. The two components can represent the two populations of AGN, steep- and flat-spectrum sources, clearly separated at low frequencies. On the contrary, at high frequencies the spectral index distribution is well fitted by only one Gaussian distribution with mean -0.25 and dispersion 0.55 , as result of the average flattening of steep-spectrum sources and the average steepening of flat-spectrum sources at high frequencies.

The spectral properties of VSA sources between 1.4 and 33 GHz can be now described by a single “two-colour diagram” using α_L and α_H (see Figure 4). There we plot open (full) points for sources with $\nu_m = 15$ (4.8) GHz; sources without 4.8-GHz measurements are indicated by a cross. Uncertainties in the spectral index are usually around 0.1 – 0.3 for both α_L and α_H ; however, they can increase more than 0.3 when α_H is calculated only by 15 and 33-GHz data (open points), due to the uncertainties associated with the VSA measurements.

The majority of sources (about $3/4$; see Table 1) are observed to change their spectral slope more than 0.3 , indicating a possible curvature in the spectrum, while very few sources can be fitted by a single power law. An average flattening in steep-spectrum sources ($\alpha_L \leq -0.5$) is still confirmed: 66% of these sources have $\Delta\alpha = \alpha_H - \alpha_L \geq 0.3$, and nearly 50% have $\Delta\alpha \geq 0.5$. From Figure 4 we notice that the largest changes in α occur for sources with $\nu_m = 15$ GHz

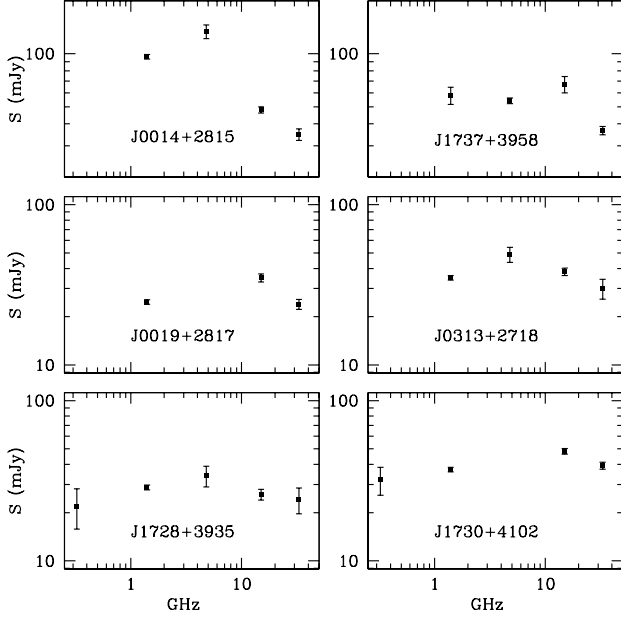


Figure 5. New GPS source candidates found in the VSA sample.

(i.e. open points or crosses): these large differences could be overestimated due to the uncertainties associated with the VSA measurements and some caution is required. In the next section, we discuss about upturn sources and we deal with this issue.

It is important to stress that few objects that are flat spectrum at GHz frequencies, keep their spectral slope flat or inverted up to 33 GHz in Figure 4. Instead, a general steepening is found. Looking at sources with $\alpha_L \sim 0$, the typical steepening is about $\Delta\alpha \simeq 0.3\text{--}0.5$. This result seems to indicate that, contrary to what normally assumed, a single power law with index $\alpha \approx 0$ is not, even statistically, a correct description of spectra for flat-spectrum sources at high frequencies. The contribution of flat-spectrum sources at the frequencies used for CMB observations could thus be lower than predicted. This is in agreement with results from Waldram et al. (2007), with recent observations by the ATCA telescope (Massardi et al. 2007; Sadler et al. 2007) and with spectral properties of WMAP sources (González-Nuevo et al. 2008).

Finally, we attempt to identify sources with spectra peaking at a frequency between 1.4 and 33 GHz, by the requirements $\alpha_L > 0$, $\alpha_H < 0$ and $\Delta\alpha < -0.3$: there are 10 sources satisfying these conditions. Only 2 of them (0024+2911 and 1526+4201) are included in the 8 GPS sources identified by C05. Six of the remaining sources could be possible GPS candidates and their spectra are plotted in Figure 5. Further data are required to confirm their GPS shape.

4 SOURCES WITH UPTURN SPECTRUM IN THE 33-GHZ VSA SAMPLE

Having previously characterised the source spectra, in this section we look for objects with upturn spectra, or in other terms, with a minimum in the spectrum at $\nu_m = 4.8$ or

15 GHz. We say that a source has an upturn spectrum if $\alpha_L < 0$ and $\alpha_H \geq 0$, in agreement with Sadler et al. (2006), but with the additional condition $\alpha_H - \alpha_L > 0.5$, in order to minimize spurious cases. Over a total of 105 sources, we find 27 objects with an upturn spectrum, corresponding to 26% of the sample (easily identified in Figure 4). While in Sadler et al. (2006) most of the objects classified as upturn are flat-spectrum at low frequencies with $\alpha_L \sim 0$, in the VSA sample there are only 8 upturn sources with $\alpha_L > -0.5$. This means that the majority of them are steep-spectrum sources at low frequencies that become flat or inverted at $\nu > 5$ GHz, with a strong variation in the spectral index (in some cases $\gtrsim 1$).

The different survey resolutions (< 1 arcmin for WENSS, NVSS and RT and ~ 3 arcmin for VSA and GB6) could affect the shape of spectra in the case of extended sources. Among the selected upturn sources, we find four that are resolved by NVSS, with the major axis between 44 and 67 arcsec. Because the RT resolution is 25 arcsec, the 15-GHz flux density could be underestimated, even if integrated fluxes are considered. In particular, two extended sources, 0010+3044 and 1240+5334, are characterized by a peculiar spectrum with a strong fall at 15 GHz ($\alpha_{4.8}^{15} < -1.5$) that could be explained if power on angular scales higher than 25 arcsec is missed by RT. Some caution is therefore needed for these objects and they are excluded from the analysis.

It is important to rule out that upturn spectra could arise from bias in the 33-GHz flux density. It is known, in fact, that for flux-limited surveys the flux density of faint sources (i.e., close to the flux limit of the survey) could be overestimated due to the Eddington bias (Eddington 1940). Using Bayes' theorem, we can calculate the maximum likelihood estimator of the flux density for a source with detected flux density S_0 (Hogg & Turner 1998; López-Caniego et al. 2007) as

$$S_{\text{ML}} = \frac{S_0}{2} \left[1 + \sqrt{1 - \frac{4\beta}{r^2}} \right] \quad \text{with } r \geq 2\sqrt{\beta}, \quad (1)$$

where r is signal-to-noise ratio of the detected flux density and β is the slope for the differential source count distribution. For the VSA sample the estimated slope is $\beta = 2.34$ (C05), implying that the Eq. 1 can be applied only to sources with signal-to-noise higher than 3 (this condition is verified by $\sim 97\%$ of the VSA sources). In the few cases where $S/N \lesssim 3$, we consider $S_{\text{ML}} = S_0/2$.

Now using the maximum-likelihood flux densities at 33 GHz we calculate the new values for α_L and α_H (the Eddington bias can be supposed negligible in the other surveys because of the high S/N ratio, at least for the VSA objects): after removing extended sources, 20 objects (19% of the sample) still verify the upturn conditions. We list them in Table 2.

As discussed by C05, there is a deliberate deficiency of bright sources in the VSA fields. The first fields to be observed were selected to avoid sources predicted to be brighter than 250 mJy at 33 GHz; later fields used a more relaxed limit of 500 mJy. As a consequence, the fields are statistically representative of the whole sky only between 20 and 46 mJy for first fields and between 20 and 114 mJy for the later fields. Limiting to $S \leq 46$ mJy we find 17 upturn sources over a total of 86, corresponding to 20%, well in agreement with

Table 2. List of VSA sources with an upturn spectrum. The flux densities are at the frequencies: 325 MHz from the WENSS; 1.4 GHz from NVSS; 4.8 GHz from GB6; 15 GHz from RT; 33 GHz from VSA. The reported spectral indices are calculated using the VSA flux densities uncorrected by the selection bias. The last column reports the frequency of the minimum in spectra, as explained in the text.

name	325 MHz	1.4 GHz	S(mJy) 4.8 GHz	15 GHz	33 GHz	α_L	α_H	$\alpha_H - \alpha_L$	ν_m GHz
0013+2834	–	39.8±1.3	23.8±3.7	28.0±2.	36.8±1.8	-0.42	0.27	0.69	4.8
0023+2928	85.±7.	41.8±1.3	26.2±5.2	20.3±2.	35.5±1.9	-0.31	0.71	1.02	15
0024+2724	318.±30.	122.7±3.7	41.4±4.1	24.0±2.	29.7±2.8	-0.73	0.27	1.00	15
0728+5325	89.±7.	60.±1.8	36.8±4.1	49.0±2.	52.9±2.7	-0.40	0.16	0.56	4.8
0728+5431	72.±7.	44.1±1.4	40.0±4.6	64.8±2.	112.4±2.7	-0.08	0.65	0.73	4.8
0931+3049	111.±8.	67.6±2.1	23.3±3.1	24.0±2.	32.6±6.7	-0.87	0.10	0.97	4.8
0944+3115	111.±8.	56.2±2.1	39.5±5.1	18.0±2.	25.3±2.6	-0.46	0.43	0.89	15
0946+3050	62.±7.	37.8±1.2	20.4±3.3	28.9±2.	28.5±2.8	-0.50	0.15	0.55	4.8
0946+3309	791.±38.	351.5±12.1	135.5±11.9	25.0±2.	40.6±2.5	-1.09	0.62	1.71	15
0950+3201	105.±7.	56.2±2.1	–	16.7±2.	21.1±3.6	-0.51	0.30	0.81	15
1215+5154	16.±6.	16.4±0.6	–	14.1±2.	26.0±6.0	-0.06	0.78	0.84	15
1219+5408	123.±8.	42.6±1.3	–	13.±2.	29.±10.	-0.50	1.02	1.52	15
1221+5429	45.±6.	36.1±1.1	14.6±3.1	32.7±2.	20.7±2.5	-0.74	0.09	0.83	4.8
1229+5147	579.±24.	175.8±5.3	41.3±4.2	41.1±2.	41.3±3.5	-1.18	0.00	1.18	4.8
1240+5441	951.±39.	223.0±6.7	59.9±6.5	20.0±2.	27.8±6.2	-1.02	0.41	1.43	15
1533+4107	53.±6.	33.4±1.4	20.4±3.4	30.±2.	28.1±2.3	-0.40	0.12	0.52	4.8
1539+4217	130.±8.	49.0±1.5	25.3±3.5	31.0±2.	34.0±1.6	-0.54	0.14	0.68	4.8
1723+4206	682.±28.	240.6±7.2	76.6±7.2	17.6±2.	24.4±2.4	-1.07	0.41	1.48	15
1733+4034	249.±12.	84.1±3.0	38.8±4.9	16.0±2.	20.8±4.4	-0.69	0.35	1.04	15
1734+3857	478.±20.	796.4±23.9	522.7±46.0	734.0±2.	939.3±1.9	-0.34	0.31	0.65	4.8

the percentage from the all sample. A smaller percentage is obtained in the area of 0.024 steradian, where there are 7 upturn sources over 43 (16%) in the range 20–46 mJy and 2 over 14 (14%) between 46 and 114 mJy.

In Figures 6–7 we show the spectra for the 20 upturn sources found in the VSA sample. For a visual inspection of spectra at low frequencies we include the flux densities at 325 MHz as measured by the Westerbork Northern Sky Survey (WENSS, Rengelink et al. 1997). We plot also the low-frequency best-fit power law: as expected for these sources, the extrapolation of the low-frequency power law to high frequencies generally underestimates the actual fluxes at 33 GHz, in some cases up to a factor of 10, like for the objects 0931+3049 and 1229+5147. It is remarkable how, in general, the flux density at 325 MHz fits well the power law extrapolation from data at frequencies about one order of magnitude higher, confirming the reliability of the power law approximation for radio spectra at low frequencies. In few cases a flattening at 325 MHz is observed, due to a possible effect of synchrotron self-absorption or a low-energy cutoff in the electron energy spectrum (Carilli et al. 1991).

An interesting case is source 1734+3857, plotted in Figure 7: it is the brightest object in the VSA sample with a flux density a bit less than 1 Jy. This source has been detected in the WMAP 23, 33, 41 and 61-GHz channels with a flux density around 1.1 Jy (Hinshaw et al. 2007; López-Caniego et al. 2007), confirming the rising spectrum at $\nu > 5$ GHz observed by the VSA measurement.

4.1 Variability in upturn sources

Since observations of the surveys were carried out at different epochs, variability of radio sources could affect the shape of spectra. A question is therefore if the observed upturn spectra could be fictitiously generated by high variability in

VSA sources. Two different cases can be discussed according to the value of ν_m .

For upturn sources with spectral minimum at $\nu_m = 15$ GHz, only the VSA flux density does not agree with a spectral power-law fit. Because observations of the RT and VSA are separated by no more than two years, such sources should be high variable in a time scale of 1–2 years, and the VSA observations should correspond to a peak in the flux density. VSA observations cover a time scale from few months up to six months. As discussed by C05, the variability of 72 sources could be examined: the majority of them (about 70%) varies by less than 25 per cent of the mean flux density, a 20% between 25 and 50 per cent and 11% more than 50 per cent. Only three upturn sources with $\nu_m = 15$ GHz are found in these 72 objects, and they show to have varied by less than 20 per cent. On the contrary, variability of at least 50 per cent is required to produce changes in the spectral index, calculated between 15 and 33 GHz, bigger than 0.5, i.e. enough to explain upturn spectra. Moreover, high variable objects are usually associated to flat-spectrum sources (see the Figure 9 of C05 where a strong correlation between variability and spectral index is found). This is confirmed by Bolton et al. (2006), who carried out a study of variability in a time scale between 1.5 and 5 years: no steep-spectrum sources have been classified as variable whilst 50 per cent of the flat-spectrum sources have varied (up to a 70% of the mean flux density). Also Sadler et al. (2006) found that at 20 GHz the general level of variability is quite low in a one-year interval, with only five sources varied by more than 30%. To conclude, it seems quite unlikely that variability could explain upturn spectra with minimum at 15 GHz.

On the other hand, the total set of data covers nearly twenty years (the GB6 survey was taken in 1986–87, WENSS in 1991–93 and NVSS between 1993 and 1996, RT in 2000–

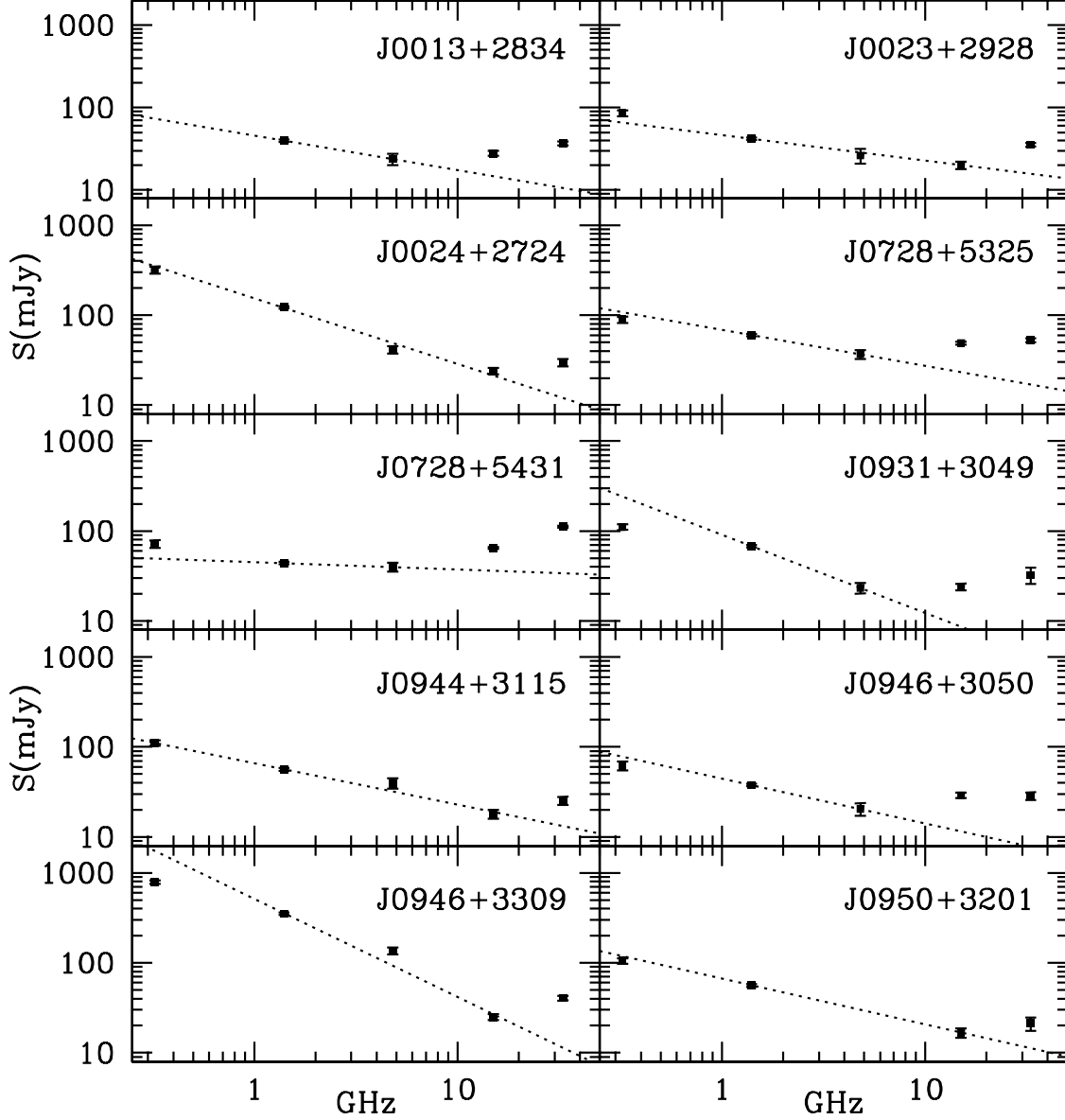


Figure 6. Sources with upturn spectra. Dotted lines are the power laws that best fit spectra at low frequencies.

2001 while VSA in 2002–03). Variability on time scales of years could be relevant for sources with spectra upturning at $\nu_m = 4.8$ GHz: because there are no observations following these sources on time scales of ten years or more, we are not able to exclude a significant long-scale variability in their flux density. We consider the “worst” case, in which the flux densities measured by GB6 at 4.8 GHz (the most distant in time from VSA measurements) correspond to a minimum in the source emission, giving a steeper low-frequency spectral index. Ignoring the 4.8-GHz fluxes, we take $\alpha_L = \alpha_{1.4}^{15}$: over the 10 upturn sources with the minimum at 4.8 GHz only 2 still satisfied our upturning conditions, even if 7 of them keep an upturn shape with the less strict conditions $\alpha_L < 0$, $\alpha_H > 0$ and $\Delta\alpha \gtrsim 0.3$. Therefore, in principle, a long-scale variability could explain the spectral curvature

observed in sources with minimum at $\nu_m = 4.8$ GHz (but not in ones with $\nu_m = 15$ GHz) requiring a large fractional variability, in many cases of the order of 100 per cent at 4.8 GHz. Because at the moment there are no observational data supporting this hypothesis and because variability is not able to explain all the upturn spectra found in the VSA sample, we are still confident that the observed upturn spectra represent intrinsic properties of radio sources. Finally, we observe that in most of upturn sources the WENSS flux densities at 325 MHz are in very well agreement with extrapolations based on the estimated α_L , indicating no variability on a time scale of years at these frequencies.

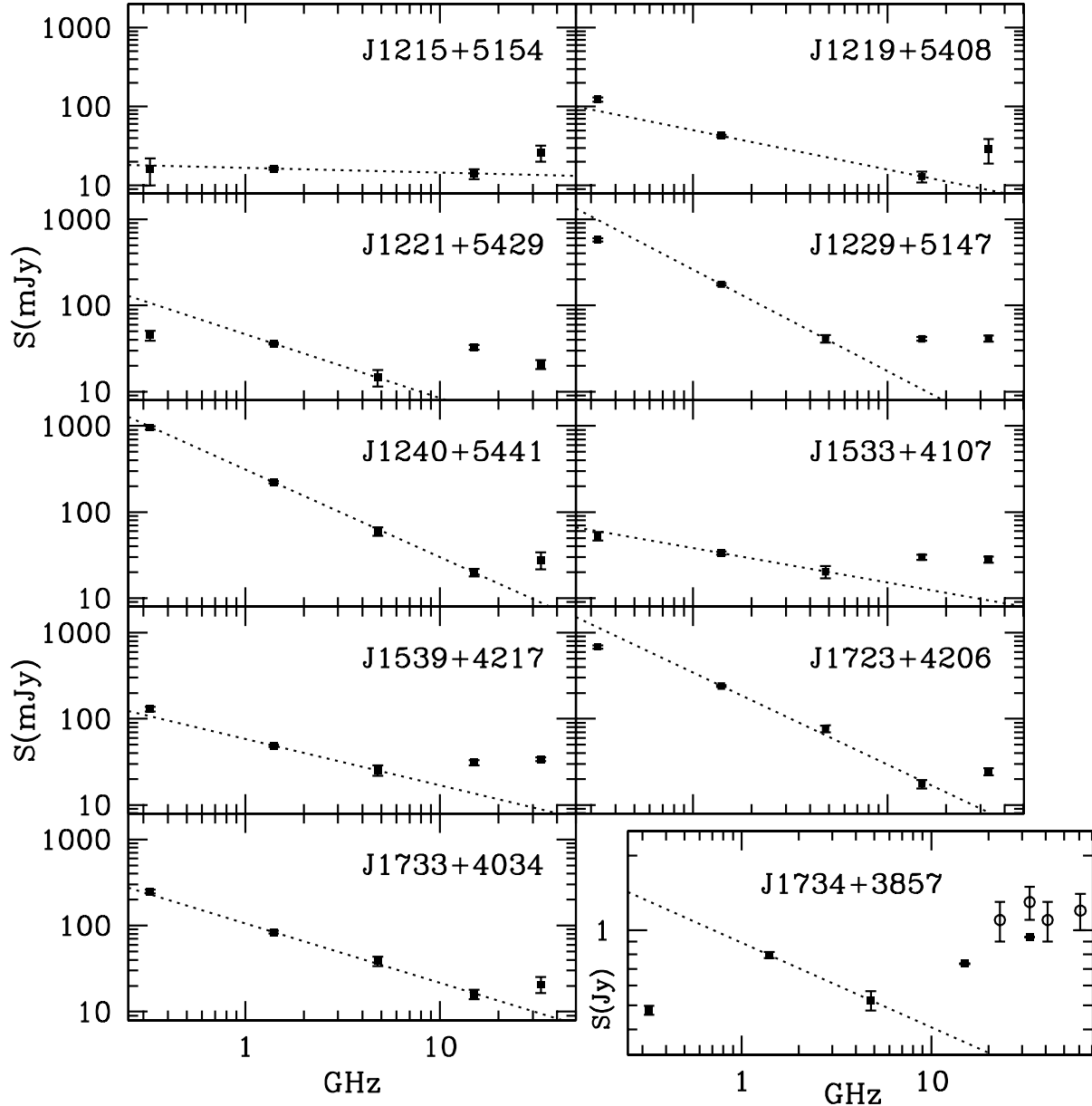


Figure 7. Sources with upturn spectra (as in Figure 6). For source 1734+3857 we plot also the flux densities obtained by López-Caniego et al. (2007) using the 3-year WMAP data (open points).

5 DISCUSSION ON FLATTENING/UPTURN SOURCES

Although not explicitly considered, sources with flattening or upturn spectra are consistent with the unified scheme for radio-loud AGNs (e.g., Orr & Browne 1982, Barthel 1989 and Urry & Padovani 1995). According to this picture, spectral properties of the AGN radio emission depend on the degree of the alignment of relativistic jets with the line of sight (hereafter the “viewing angle”): in a simplistic way, steep spectra are observed in misaligned objects, where radio emission is dominated by extended optically-thin lobes; on the other hand, if the line of sight is enough close to the AGN jet, the optically-thick and beamed emission of the AGN compact core emerges with the typical flat spectrum

(Peacock 1985). The critical viewing angle θ_c that defines the division between flat- and steep-spectrum objects at GHz frequencies is usually considered around 10° for quasars and 30° for BL Lacs (Ghisellini et al. 1993; Jackson & Wall 1999). Therefore, for angles θ not much larger than θ_c , we expect a transition from steep to flat spectra at some frequency $\nu \gtrsim 5$ GHz, when the compact emission begins to dominate over the extended one (whose spectrum falls rapidly with the frequency). Jackson & Wall (1999) employed this idea in order to extrapolate the number counts of radio sources at 151 MHz to 5 GHz, introducing the “beamed” contribution of parent populations of blazars. This picture is in agreement with high-resolution observations: AGN radio structures are commonly resolved into three basic components (nuclear core, large scale jets and outer lobes), while ex-

tended radio structures without a contribution from a core are rare (Pearson & Readhead 1988). Moreover, the relative importance of the AGN core emissions is observed to increase at higher and higher frequencies (see, e.g., Bach et al. 2004 for Cygnus A and Kharb et al. 2007 for a sample of Fanaroff-Riley II).

Now we discuss more quantitatively how the unified scheme applies to our case. We consider the observed flux density of VSA sources to be the sum of two components, an extended steep-spectrum and a flat-spectrum core-dominated emission. For simplicity, we suppose that the VSA sample is composed of quasars, being the dominant population at that frequency and flux range. Let R_c^{obs} be the observed core-to-extended flux ratio at 5 GHz. At a frequency $\nu > 5$ GHz the core component dominates the total emission if

$$R_c^{obs} = \left(\frac{S_c}{S_{ext}} \right)_{5 \text{ GHz}} > \left(\frac{\nu}{5 \text{ GHz}} \right)^{\alpha_{ext} - \alpha_c}, \quad (2)$$

where α_{ext} and α_c are the spectral index of the two components, extended and compact. In the following, we adopt as spectral indices the typical values for steep- and flat-spectrum sources at low frequencies, $\alpha_{ext} = -0.75$ and $\alpha_c = -0.1$ (De Zotti et al. 2005). The value for α_{ext} could be conservative at frequencies $\nu > 10$ GHz because it does not take into account possible steepening due to the electron ageing.

Objects with flattening or upturn spectrum in the VSA sample should be characterized by $S_c/S_{ext} > 1$ at 33 GHz, corresponding to $R_c^{obs} > 0.3$. A relevant fraction of them, moreover, shows flattening/inverted spectra already at 15 GHz, requiring $R_c^{obs} > 0.5$. If the core emission comes out from a relativistic jet of bulk velocity βc , the observed flux density is Doppler-enhanced by $\delta^{p-\alpha_c}$, where $\delta = [\gamma(1 - \beta \cos \theta)]^{-1}$ is the Doppler factor and $\gamma = (1 - \beta^2)^{-1/2}$ is the Lorentz factor. The parameter p depends on the emission model and is equal to 3 for a moving, isotropic source and 2 for a continuous jet (see Ghisellini et al. 1993 and Urry & Padovani 1995 for a detailed discussion). Then, the relation between the observed (R_c^{obs}) and the intrinsic-unbeamed (f) core-to-lobe flux ratio for a source at redshift z is given, after the K-correction, by

$$R_c^{obs} = f \delta^{p-\alpha_c} (1+z)^{\alpha_c - \alpha_{ext}}. \quad (3)$$

In the unified scheme, the value of f is the same for quasars and for their parent population, the FR II galaxies. Because there is no evidence that the parameter f correlates with the radio power of FR II galaxies (Jackson & Wall 1999), we can use the best-fit FR II value $f = 5 \times 10^{-3}$ (Urry & Padovani 1995) for both steep- and flat-spectrum quasars, independently of their luminosity.

Using Eq. 3, now we are able to provide an indicative estimate of R_c^{obs} for quasars observed at a viewing angle $10^\circ \leq \theta \leq 20^\circ$: supposing a Lorentz factor between 2 and 15, we obtain

$$\begin{array}{llll} \theta = 10^\circ & \delta = [3.4, 5.7] & R_c^{obs} = [0.3, 1.5] & p = 2 \\ & & R_c^{obs} = [1.0, 8.3] & p = 3 \\ \theta = 15^\circ & \delta = [1.8, 3.7] & R_c^{obs} = [0.05, 0.4] & p = 2 \\ & & R_c^{obs} = [0.09, 1.5] & p = 3 \\ \theta = 20^\circ & \delta = [1.1, 2.7] & R_c^{obs} = [10^{-2}, 0.15] & p = 2 \\ & & R_c^{obs} = [10^{-2}, 0.4] & p = 3 \end{array} \quad (4)$$

The K-correction is of little relevance, being a factor ~ 1.6 for $z = 1$ (the redshift we use). Fixing the viewing angle and for the considered parameters, the value of R_c^{obs} scatters over a range of a factor 30. In any case, we note that for $\theta = 10^\circ$ R_c^{obs} is compatible with the values required to have an upturn spectrum, independently of the γ and p used. This is not the case when θ is near to 20° (which should be considered as upper limit) and upturn spectra are possible only for low values of the Lorentz factor ($\gamma \lesssim 5$) and $p = 3$. The case of $\theta = 15^\circ$ may be more conservative because the condition that $R_c^{obs} = 0.3$ is verified independently of p , at least for $\gamma \lesssim 10$. Therefore, according to this model and for the range of frequencies investigated, a viewing angle of $\theta \lesssim 15^\circ$ is required to observe quasars with a flattening spectrum.

5.1 Predicted number of flattening/upturn sources in the VSA sample

A prediction of how many upturn sources should be expected in a sample selected at 33 GHz is quite difficult, not only for the scattering in the physical parameters used in Eq. 3, but also for selection effects in flux-limited samples. However, following the previous discussion, a qualitative estimate is possible. We want to stress that nearly all the VSA upturn sources (18/20) have $\alpha_L < -0.3$. Sources with $-0.5 < \alpha_L < -0.3$, although not strictly steep spectrum according the usual definition, can be considered a transition between lobe- and core-dominated quasars. In the following we do not make a distinction between them.

We suppose that all the sources with steep spectra at low frequencies observed at viewing angles $10^\circ \leq \theta \leq 15^\circ$ show a flattening or rising spectrum at $\nu \gtrsim 5$ GHz. If lobe-dominated quasars are in general observed at $10^\circ \leq \theta \leq 40^\circ$ (Ghisellini et al. 1993), we should find that about 1/6 of steep-spectrum sources have a flattening or upturn spectrum at high frequencies (in the hypothesis that the probability to observe a radio quasars is independent of θ). This estimate should be only applied to samples selected at few GHz. In flux-limited samples selected at high frequencies, this percentage could be higher because of missing very steep spectrum sources. As example, in the VSA sample we have found 18 upturn objects out of a total of 69 sources which are steep ($\alpha_L < -0.3$) at low frequencies.

In order to establish if the number of flattening/upturn sources expected from the model is in agreement with the number observed in the VSA sample, we proceed in the following way:

- we suppose that for flattening/upturn sources the average “high-frequency” spectral index is $\langle \alpha_H \rangle = 0$.
- Using the NVSS and GB6 surveys we select inside the VSA fields all sources with $\alpha_{1.4}^{4.8} < -0.3$ and flux density higher than 20 mJy at 4.8 GHz. We find 370 objects.
- Extrapolating the flux density to 15 GHz using $\alpha_{1.4}^{4.8}$, we find that 149 of these 370 sources have $S_{15} \geq 20$ mJy. According to the above discussion, we expect that 1/6 of them (i.e. 25 objects) have flat or inverted spectrum at high frequencies ($\alpha_H \sim 0$), and are observed in the VSA sample.
- Moreover, the rest of the 221 steep-spectrum sources (with $S_{4.8} \geq 20$ mJy but the extrapolated $S_{15} < 20$ mJy) can also be observed in the VSA sample if their spectra are

flat starting from $\nu = 4.8$ GHz. These objects correspond to the previous cases with $\nu_m = 4.8$ GHz, and they are more or less one half of the total number of flattening/upturn sources. Therefore, considering a fraction of 1/12, we have a further contribution of 18 objects.

To resume, the number of sources with flattening/upturn spectrum predicted by our estimates in the VSA area at 33 GHz is 43. This value should be compared with the number of steep-spectrum ($\alpha_L < -0.3$) sources with $\Delta\alpha = \alpha_H - \alpha_L \geq 0.3$ found in the VSA sample. This difference is in fact approximately the change of the spectral index in the case $S_c > S_{ext}$ at 33 GHz (using the α_c and α_{ext} assumed above). As seen in Table 1, there are 43 sources with these characteristics, as from our predictions. A smaller number, 37, is found if we correct the 33-GHz VSA flux densities by the Eddington bias.

If we want to limit our predictions only to sources with an upturn behaviour, i.e. rising at high frequencies, we should require that $\alpha_c > 0$ and $S_c \gg S_{ext}$ at 33 GHz. The fraction of flat-spectrum sources with $\alpha > 0$ can be obtained from samples of sources whose emission is dominated by the AGN compact core: Ricci et al. (2006) showed that for a complete sample of flat-spectrum sources at 5 GHz, the distribution of the spectral index calculated between 2.7 and 5 GHz is well described by a Gaussian with $\langle\alpha\rangle = -0.1$ and $\sigma_\alpha = 0.3$. These values are similar to parameters describing the spectral index distribution at low frequencies for flat-spectrum sources in the VSA sample (see Figure 3). Using these parameters in a Gaussian distribution, we find that about 38 per cent of spectral indices are higher than 0. This means that 16 of the 43 predicted objects with flattening spectrum is expected to be upturn between 5 and 33 GHz, again in agreement with the results from the VSA sample.

6 UPTURN SOURCES FROM HIGH-FREQUENCY SURVEYS

In this section we search for sources with upturn spectra in other surveys at frequencies comparable or higher than the VSA one. The fraction of “upturn” sources is expected to depend on the selection frequency and the flux-density range of surveys (Kellermann et al. 1968). A direct comparison with the VSA results should take into account this.

- **WMAP source catalogue.** The WMAP mission has produced the first all-sky surveys of extragalactic sources at 23, 33, 41, 61 and 94 GHz and at Jy flux densities (Bennett et al. 2003; Hinshaw et al. 2007). In this interval of frequencies, spectral properties of extragalactic sources are still poorly investigated. From 3-years WMAP maps, Hinshaw et al. (2007) provided a catalogue of 323 objects above a flux limit of about 1 Jy. This catalogue was improved by López-Caniego et al. (2007) using a non-blind method based on the second member of the Mexican Hat Wavelet Family. They found 368 sources with a 5- σ detection in at least one WMAP channel and with a completeness flux limit of around 1.1 Jy.

We complement the WMAP flux densities by measurements from low-frequency surveys: in the northern hemisphere from the NVSS and GB6 surveys; in the southern hemisphere from the SUMSS (Mauch et al. 2003) and PMN

(Wright et al. 1994; Wright et al. 1996) surveys at 843 MHz and 4.85 GHz respectively. We use these data to define the low-frequency spectral index (α_L) for WMAP sources. Objects without a counterpart both in NVSS/SUMSS and in GB6/PMN or without a clear identification have been discarded from the analysis: 248 objects remain, 114 with low-frequency spectral index $\alpha_L < 0$ and only 22 with $\alpha_L \leq -0.5$. If the high-frequency spectral index is calculated between 4.8 GHz and the lowest frequency at which a source has been detected by WMAP, we find 25 upturn sources (5 with $\alpha_L \leq -0.5$) according to the previous definition. Some examples of these with counterparts in the multi-frequency catalogue by Kuehr et al. (1981) or in the ATCA observations (Ricci et al. 2006; Massardi et al. 2007) are shown in Figure 8.

The detection of objects with upturn spectrum in the WMAP catalogue is an important confirmation of the presence of this class of sources also at Jy flux levels. Their fraction is about 10%, lower than in the VSA sample. This is not unexpected due to the different range of flux densities considered by the two experiments. At Jy level, in fact, the source population is dominated by flat-spectrum sources (De Zotti et al. 2005) and the fraction of objects with inverted spectrum at low frequency is particularly high. In the WMAP catalogue more than 50% of sources have $\alpha_L > 0$, compared to 17% in the VSA sample.

For a better comparison between the two samples we consider only the WMAP sources with a 5- σ detection in the 33-GHz channel, in order to achieve a sample selected at the same frequency of the VSA. Then, we compute α_L and α_H as in section 3.1 (using the 23-GHz WMAP channel instead of the 15-GHz frequency). Now, if we limit the comparison only to objects with decreasing spectrum at low frequency ($\alpha_L < 0$), we find about 20% of upturn sources in the WMAP catalogue, very close to 23% in the VSA sample.

- **The 20 GHz ATCA Survey.** A pilot survey of the Australia Telescope 20 GHz survey was presented by Sadler et al. (2006), consisting of a flux-limited sample ($S \geq 100$ mJy) of 173 radio sources selected at 20 GHz, including near-simultaneous flux measurements at 4.8, 8.6 and 18 GHz. In the paper, using also the flux densities provided by the SUMSS catalogue (Mauch et al. 2003), they carried out an accurate analysis of source spectra in the frequency range 0.8–20 GHz: about 20% of source spectra were classified upturn (defined as $\alpha_{0.8}^5 < 0$ and $\alpha_{8}^{18} > 0$). However, introducing our stricter condition that $\alpha_{8}^{18} - \alpha_{0.8}^5 \geq 0.5$, the fraction is reduced to 14%.

Recently, a complete sample of bright sources ($S_{20GHz} > 0.5$ Jy), carried out with ATCA, was presented by Massardi et al. (2007). For 218 of them, near simultaneous observations at 4.8, 8.6 and 20 GHz were also provided. Massardi et al. (2007) studied the source spectral behaviour in the frequency range 5–20 GHz: a general steepening in spectra is observed, while very few upturn sources are found (only three according our definition; see their Figure 4). Extending the analysis to the NVSS and SUMSS measurements at 1.4 and 0.8 GHz, the number of sources with upturn spectra increases to 19 (8% of the sample), indicating that their spectral minimum is at $\lesssim 5$ GHz. However, as for the WMAP case, if we exclude objects with inverted spectrum at low frequency (that are about 60% of the sample), the fraction of

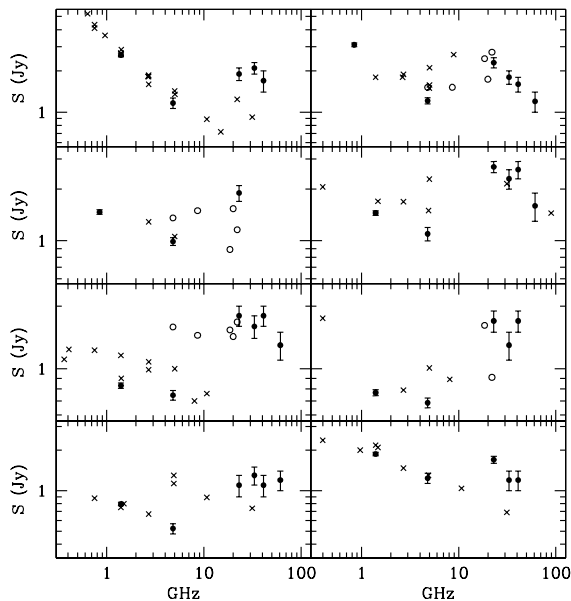


Figure 8. Examples of upturn spectra in the WMAP catalogue. Counterparts in the Kuehr et al. (1981) and in the ATCA samples are shown as cross points and open squares respectively. Full points are from WMAP and from SUMSS/NVSS and PMN/GB6 at low frequencies.

upturn sources is of the order of 20%, well in agreement with the VSA and WMAP one.

• **Radio follow-up of the 9C survey.** Bolton et al. (2004) carried out a follow-up of 176 sources from the 15-GHz 9th Cambridge survey in the frequency range [1.4, 43] GHz. In particular, they made simultaneous measurements at 1.4, 4.8, 22 and 43 GHz with the VLA and at 15 GHz with the Ryle Telescope. As discussed by the authors (see also Waldram et al. 2007), there is a clear trend for spectra to be steeper at the high frequencies: an average steepening is already observed at 22 GHz, but it becomes especially strong in the range 15–43 GHz (the median spectral index is -0.89), with a large number of objects with extremely steep spectra, less than -1.5 . We find only 22 (14%) inverted sources between 4.8 and 22 GHz and very few objects inverted up to 43 GHz or upturn.

This strong steepening at $\nu > 15$ GHz has not been observed in other surveys (ATCA measurements found a steepening in 20–95 GHz spectral indices, however the median values is -0.39 ; see Sadler et al. 2007) and it is clearly in disagreement with VSA results. Such a discrepancy may be related to the different resolution of the instruments, e.g. a few arcsec for the VLA at 22–43 GHz, 25 arcsec for the Ryle Telescope and just 3 arcmin for the VSA source subtractor.

7 DISCUSSION AND CONCLUSIONS

An accurate control of the contribution of extragalactic radio sources at microwave wavelengths will be extremely important for future CMB experiments at arcminute resolution like Planck and for experiments aimed to the detection of the cosmological B-mode polarization (Tucci et al. 2005). The

VSA source-subtractor observations provide a very useful nearly-complete catalogue of “faint” (20–100 mJy) extragalactic radio sources at a frequency used for CMB measurements. In this paper, using additional measurements at lower frequencies, we investigate the spectral properties of the VSA catalogue in the frequency range 1.4–33 GHz.

The most interesting result we find is related to the high-frequency spectral behaviour of sources whose spectrum is steep at GHz frequencies. Typical models for this source population (see, e.g., the recent work by De Zotti et al. 2005) predict a spectral steepening at high frequencies due to the rapid ageing of high-energy electrons, responsible of the emission at $\nu \gg 1$ GHz. On the contrary, from the 33-GHz VSA catalogue we observe that the spectrum of the majority of them flattens or even becomes inverted at $\nu \gtrsim 5$ GHz. In particular, in about 50 per cent of steep-spectrum sources the spectral flattening at high frequencies is more than 0.5. Moreover, we find objects with upturn spectra, i.e. steep at low frequencies but rising between $5 < \nu < 33$ GHz: 20 sources clearly show such spectral behaviour, corresponding to 19 per cent of the total sample.

The large fraction of sources characterized by spectral flattening and the lack of correlation between flux density and spectral curvature are indications that we are observing intrinsic properties of radio sources, and not the result of selection effects or bias. Variability can affect the shape of spectra observed in measurements that are not simultaneous. However, it is quite unlikely that variability is responsible of the average spectral flattening found in VSA steep-spectrum sources. In fact, it would require large variations in flux densities on time scales of both 1–2 years and a decade, for a source population usually observed to exhibit little variability (see, e.g., Sadler et al. 2006, Bolton et al. 2006).

In the paper, we show that source spectra with flattening or upturn behaviour are completely consistent with the “unified model” for AGNs: steep spectra in radio sources can be physically understood as emission from extended optically-thin radio lobes, while a flat-spectrum component arises from the central compact and optically-thick core of radio sources. Due to the rapid decrease in intensity of the diffuse emission with frequency, the emission from the compact core of AGNs may start to dominate at frequency $\nu \gg 1$ GHz if the radio jet axis lies enough close to the line of sight (Jackson & Wall 1999). According to the typical physical parameters for quasars, it can occur for $\nu \gtrsim 5$ GHz when the viewing angle is $\theta \lesssim 15^\circ$.

Finally, VSA data confirm that a simple power-law extrapolation of low-frequency flux densities to mm wavelengths is not reliable: this is not only because a fraction of sources predicted at high frequencies are not found, but also because a significant number of sources that would not be expected are detected. For example, using a simple extrapolation of the spectral slope between 1.4 and 4.8 GHz to 33 GHz, we find that 34 sources present in the VSA catalogue would be predicted to be fainter than the flux limit of 20 mJy and not included in the sample. From surveys in literature, the percentage of these “unexpected” objects is observed to steadily increase with the frequency. While it is roughly 10% at 15 GHz (see Taylor et al. 2001) and 18% at 20 GHz (see Sadler et al. 2006), this percentage increases up to 32% in the VSA sample.

We conclude that radio sources with flattening or upturn spectrum could be an important contaminant to high-resolution CMB observations providing to an extra contribution to source number counts respect to predictions based on surveys at 1–5 GHz. At 33 GHz this extra contribution is not negligible: limited to the 20 upturn sources found in the VSA sample, we substitute their measured flux density with the one obtained from a low-frequency extrapolation; in this case, the VSA number counts at 33 GHz would keep the same slope as found by C05 but rescaled down by 15 per cent. This is for flux densities $20 \leq S \lesssim 100$ mJy. At higher fluxes the fraction of upturn sources is observed to be lower, around 10 per cent in the WMAP and ATCA source catalogues at Jy levels. If confirmed, it would suggest an extra contribute from upturn sources of about 10–15% to temperature fluctuations generated by extragalactic radio sources at 33 GHz. At higher frequencies the relevance of this class of sources is expected to increase.

In the near future a number of new ground-based surveys at 20–30 GHz will be available, as, for example, the super-extended version of VSA, the Australia Telescope 20 GHz survey and the One Centimetre Receiver Array (OCRA) project. They will be able to more deeply investigate radio source spectra in large intervals of fluxes and to confirm the results discussed in this paper. However, observations at frequencies higher than 30 GHz are required for a better characterization of upturn sources. In this sense, the ESA’s Planck satellite will be extremely important, carrying out all-sky surveys from 30 to 860 GHz with a sensitivity several times better than WMAP, and extending high-frequency radio surveys to fluxes of few hundred of mJy.

Acknowledgements. MT thanks to Luigi Toffolatti for the careful reading of the manuscript and helpful comments and Elizabeth WalDRAM for the useful discussions.

REFERENCES

- Bach U., Krichbaum T.P., Middelberg E., Kadler M., Alef W., Witzel A., Zensus J.A., 2004, Proceedings of the “7th Symposium of the European VLBI Network on New Developments in VLBI Science and Technology”, p.155–156.
- Barthel P.D., 1989, *ApJ*, 336, 606.
- Bennett C.L., Hill R.S., Hinshaw G., et al., 2003, *ApJS*, 148, 97.
- Bolton R.C., Cotter G., Pooley G.G., Riley J.M., WalDRAM E.M., Chandler C.J., Mason B.S., Pearson T.J., Readhead A.C.S., 2004, *MNRAS*, 354, 485.
- Bolton R.C., Chandler C.J., Cotter G., Pearson T.J., Pooley G.G., Readhead A.C.S., Riley J.M., WalDRAM E.M., 2006, *MNRAS*, 370, 1556.
- Carilli C.L., Perley R.A., Dreher J.W., Leahy J.P., 1991, *ApJ*, 383, 554.
- Cleary K.A., Taylor A.C., WalDRAM E., et al., 2005, *MNRAS*, 360, 340 (C05);
- Cleary K.A., Taylor A.C., WalDRAM E., et al., 2008, submitted to *MNRAS* (Erratum).
- Condon J. J., Cotton W. D., Greisen E. W., Yin Q. F., Perley R. A., Taylor G. B., Broderick J. J., 1998, *AJ*, 115, 1693.
- De Zotti G., Ricci R., Mesa D., Silva L., Mazzotta P., Toffolatti L., González-Nuevo J., 2005, *A&A*, 431, 893.
- Dickinson C., Battye R.A., Carreira P., et al., 2004, *MNRAS*, 353, 732.
- Dunlop J.S., Peacock J.A., 1990, *MNRAS*, 247, 19.
- Eddington A.S., 1940, *MNRAS*, 100, 354.
- Ghisellini G., Padovani P., Celotti A., Maraschi L., 1993, *ApJ*, 407, 65.
- González-Nuevo J., Massardi M., Argüeso F., Herranz D., Toffolatti L., Sanz J.L., López-Caniego M., de Zotti G., 2008, *MNRAS*, 384, 711.
- Grainge K., Carreira P., Cleary K., et al., 2003, *MNRAS*, 341, L23.
- Gregory P. C., Scott W. K., Douglas K., Condon J. J., 1996, *ApJS*, 103, 427.
- Hinshaw G., Nolta M.R., Bennett C.L., et al., 2007, *ApJS*, 170, 288.
- Hogg D.W., Turner E.L., 1998, *PASP*, 110, 727.
- Jackson C.A., Wall J.V., 1999, 304, 160.
- Jones M.E., 1991, in Cornwell T.J., Perley R., eds., *Proc. IAU Colloq. 131, ASP Conf.Ser. 19, Radio Interferometry. Theory, Techniques, and Applications*, Astron. Soc. Pac., San Francisco, p.395.
- Kellermann K.I., Pauliny-Toth I.I.K., Davis M.M., 1968, *ApL*, 2, 105.
- Kharb P., O’Dea C., Baum S., Daly R., Mory M., Donahue M., Guerra E., 2007, *astro-ph/0702009*.
- Kuehr H., Witzel A., Pauliny-Toth I.I.K., Nauber U., 1981, *A&AS*, 45, 367.
- López-Caniego M., González-Nuevo J., Herranz D., Massardi M., Sanz J.L., De Zotti G., Toffolatti L., Argüeso F., 2007, *ApJS*, 170, 108.
- Massardi M., Ekers R.D., Murphy T., et al., 2007, *astro-ph/0709.3485*.
- Mauch T., Murphy T., Buttery H.J., Curran J., Hunstead R.W., Piestrzynski B., Robertson J.G., Sadler E.M., 2003, *MNRAS*, 342, 1117.
- O’Dea C.P., 1998, *PASP*, 110, 493.
- Orr M.J.L., Browne I.W.A., 1982, *MNRAS*, 200, 1067.
- Partridge B., et al., 2007, in preparation.
- Peacock J.A., 1985, *MNRAS*, 217, 601.
- Pearson T.J., Readhead C.S., 1988, *ApJ*, 328, 114.
- Rengelink R.B., Tang Y., de Bruyn A.G., Miley G.K., Bremer M.N., Roettgering H.J.A., Bremer M.A.R., 1997, *A&AS*, 124, 259.
- Ricci R., Sadler E.M., Ekers R.D., Staveley-Smith L., Wilson W.E., Kesteven M.J., Subrahmanyan R., Walker M.A., Jackson C.A., De Zotti G., 2004, *MNRAS*, 354, 305.
- Ricci R., Prandoni I., Grupponi C., Sault R.J., De Zotti G., 2006, *A&A*, 445, 465.
- Sadler E.M., Ricci R., Ekers R.D., et al., 2006, *MNRAS*, 371, 898.
- Sadler E.M., Ricci R., Ekers R.D., Sault R.J., Jackson C.A., De Zotti G., 2007, *astro-ph/0709.3563*.
- Taylor A.C., Grainge K., Jones M.E., Pooley G.G., Saunders R.D.E., WalDRAM E.M., 2001, *MNRAS*, 327, L1.
- Trushkin S.A., 2003, *Bull. Spec. Astrophys. Obs.*, 55, 90.
- Toffolatti L., Argüeso F., De Zotti G., Mazzei P., Franceschini L., Danese L., Burigana C., 1998, *MNRAS*, 297, 117.
- Toffolatti L., Negrello M., González-Nuevo J., de Zotti G., Silva L., Granato G.L., Argüeso F., 2005, *A&A*, 438, 475.
- Tucci M., Martínez-González E., Toffolatti L., González-

- Nuevo J., De Zotti G., 2004, MNRAS, 349, 1267.
- Tucci M., Martínez-González E., Vielva P., Delabrouille J., 2005, MNRAS, 360, 935.
- Urry C.M., Padovani P., 1995, PASP, 107, 803.
- Waldram E.M., Pooley G.G., Grainge K.J.B., Jones M.E., Saunders R.D.E., Scott P.F., Taylor A.C., 2003, MNRAS, 342, 915.
- Waldram E.M., Bolton R.C., Pooley G.G., Riley J.M., 2007, MNRAS, 379, 1442.
- Watson R.A., Carreira P., Cleary K., et al., 2003, MNRAS, 341, 1057.
- Wright A.E., Griffith M.R., Burke B.F., Ekers R.D., 1994, ApJS, 91, 111.
- Wright A.E., Griffith M.R., Hunt A.J., Troup E., Burke B.F., Ekers R.D., 1996, ApJS, 103, 145.